有限元素法應用於具脫層複合材料的挫曲行為分析

蔡國忠[1] 盧信維[2]

1. 國立宜蘭技術學院機械工程系副教授
2. 國立宜蘭技術學院機械工程系畢業生

摘 要

疊層複合材料的結構會因為製造的缺陷或因外物衝擊而產生層與層之間的分離，這種層與層之間的分離稱為脫層。具脫層的複合材料結構體對於壓力的抵抗會隨著脫層的大小而降低。當壓力大到某一定值時，複合材料會產生挫曲。在此篇論文裏，三度空間的有限元素分析法用來分析此種脫層複材的挫曲行為，不同的脫層位置及形狀皆被研究以明瞭這些變化對於複材挫曲行為的影響。同時，非線性的接觸元素被用來模擬脫層的地方。分析的結果與從已發表的實驗結果比較非常地吻合，故此法可以用來預測脫層複材的挫曲行為。

關鍵詞： 疊層複合材料、脫層、挫屈、有限元素分析法、及接觸元素

The Buckling Behavior Analysis of the Delaminated Composites by Using the Finite Element Method

Gwo-Chung Tsai[1] and Shing-Wei Lu[2]

1. Associate Professor, Department of Mechanical Engineering, National I-Lan Institute of Technology
2. Graduate, Department of Mechanical Engineering, National I-Lan Institute of Technology

Abstract

The laminate composite structure is easily to lose the bonding between laminas due to the manufacture defect, or impacted by the outside objects .The de-bonding between the plys observed in the laminate composite is called de-lamination. The resistance capability against the compression force for the laminated composite is going down very much. The raising compression force applied to the delaminated composite structure will cause the buckling phenomena. In this paper, 3-D finite element method is applied to analyze the buckling problems of the delaminated composite. Different delaminated locations and lengths of composite laminate were studied. The nonlinear contact elements at the locations of de-lamination are applied. The published experimental data were used to check the analytical results. Good agreements were obtained between the finite element analyses and experimental results.

Key Words：The laminate composite, de-lamination, buckling, finite element analyses, and contact element

I. Introduction

De-lamination represents the interface de-bonding between the plys. Generally, de-lamination is a part of de-bonding interface, the causes of the de-bonding are very complicated and its location may be different. Sometime, the de-bonding is located at the center of the composite laminate or its edge. The de-bonding shape may be rectangular, circle, or elliptic, or irregular. For simply analyzing the buckling behavior of the structure with different delaminated shape, the regular de-lamination shape such as circle, rectangular, or elliptic are assumed. The strength of delaminated composite under the tensional force is unaffected that it is almost the same as the strength of the composite laminate without any damage. But, the compressive or buckling strength of delaminated composite is reduced so much. Therefore, the buckling phenomena are attracted lots of researches to do these investigations [Refs.1-20]. Generally, if the composite laminate plate without any defect inside, it will have the deformation under the compression force; when the external fore is increased up to a critical value, the composite laminate plate will produce the global buckling. If the composite laminate has the de-laminations, the composite laminate will produce the local buckling at the location of delaminating area or mixed buckling as shown in Figure 1 [3].

For composite laminate with de-laminations, the local buckling or mixed buckling will be observed early than the global buckling. Due to the de-lamination, the capability of resisting the compression force will be lower. Reducing the compression resistance capability of the composite laminate will depend on the area of the de-lamination, the shape of the de-lamination, and the location of the de-lamination.

When the composite laminate with the de-lamination was subjected to the external force, the composite laminate will have the buckling. At this time, the structure still can resist the external force until the de-lamination started to propagate.
To determine the critical buckling load is very important when the composite laminate with compression force. Also the post buckling behavior of the laminate composite and the mode of the de-lamination propagation are also important for completely understanding the buckling behavior of the laminate composite beam or plate.

In this paper, the complicated de-lamination shapes are considered to investigate its effect on the buckling load of the laminate composite. Due to the complicated geometry, the finite element method is used to perform the analysis. It also showed that the critical buckling load obtained from the theoretical analysis is the same as the results obtained from the finite element analysis for a simple column. The complicated de-lamination area in the composite laminate investigated in this paper will have circle area, triangular area, and rectangular area. Using the contact element modifies the de-lamination area and nonlinear buckling analyses are performed in this study.

II. Theoretical Analysis Background

Consider the buckling problem of a continuous column. The buckling problem is governed by the following differential equations:

$$\frac{d^2}{dx^2}\left[EI(x)\frac{d^2w}{dx^2}\right]+p\frac{d^2w}{dx^2}=0 \qquad .(1)$$

Where w(x)=transverse displacement; x=axial coordinate; E=modulus of elasticity; I(x)=moment of inertia; and P is compressive load at one and of the column.

The supports were shown in Figure 2. Thus the boundary conditions will be

$$w(0)=w(L)=0 \qquad (2)$$

$$w''(0)=w''(L)=0 \qquad (3)$$

The buckling load and the associated buckling mode can be obtained through solving the above differential equation (1), with the boundary conditions in (2) and (3), which together give a boundary value problem. The critical load, P_{cr}, may have the form:

$$P_{cr} = \frac{p^2 EI}{AL^2} \tag{4}$$

1. Finite Element Analysis

For simple column, the critical buckling load can be calculated from Equa.(4). The beam or plate with different geometrical location and shape of de-lamination are solved through the finite element analysis. The buckling load and mode can be analyzed and generally two different buckling analyses are considered: (1) linear buckling analysis; and (2) nonlinear buckling analysis.

A linear buckling analysis is a simple method to get the critical buckling load. In this method, the bifu rcation point can be found with the co-existed conditions between the compression condition and the buckling condition as shown in Figurer 3. After bifurcation point was found, the problem can be transferred to be the eigenvalue-eigenvector problem. The analysis can be called eigenvalue buckling analysis.

For a simple beam under the two applied forces shown in Fig.4, one is the axial force, F_o, the other is the transverse F_v ,

The governing equation can be written to be the following [3]:

$$([k]+ë[s])\{Ø\}=\{f\} \tag{5}$$

where [k] is the stiffness matrix; [s] is the stress stiffens matrix (caused by F_o), {Ø} is the transverse displacement vector; { f } is the force vector, and ë is a scale factor or called eigenvalue, sometime it is called load factor. Two cases are considered in here: (1)if F_o is a tension load ($F_o>0$), the stress stiffness matrix [s] will be a positive value, the stiffness of the beam will be improved in the transverse direction. The transverse displacement will be smaller than that without the tension load. (2) If F_o is a compression force ($F_o<0$). The structure will have the negative stress stiffness matrix, [s]. The stiffness of the column in the transverse direction will become weak. If F_o continue going up, the stiffness weakness effect in the transverse direction will become bigger. When the axial compression is continuing increasing, the stiffness of the structure is going to decrease. When the stiffness of structure became zero, the structure will be buckled. At the time of the buckling condition, ë will be called $ë_{cr}$, and the corresponding compression load, F, can become the buckling load, $F_{cr}=ë_{cr} F_o$. The eigenvector, {Ø} corresponding to the buckling load will be the buckling mode of the structure.

The buckling behavior of the structure will be observed when the compressible axial load will reduce the stiffness of the structure and reached to zero stiffness. At this time the deflection in the transverse direction will be increased to a very higher values. Therefore, the analysis of the buckling of the structure have to find the negative stiffness matrix of the structure, then find the critical buckling load in advance. The figure 5 is shown that three components of loading N_x, N_y, and N_{xy} are applied to plate.

The negative stiffness matrix can be derived in the following. The relationship between the stress and the loading can be expressed

$$\left.\begin{aligned} N_x &= \int_{-H/2}^{H/2} s_x \, dz \\ N_y &= \int_{-H/2}^{H/2} s_y \, dz \\ N_{xy} &= \int_{-H/2}^{H/2} s_{xy} \, dz \end{aligned}\right\} \quad .(6)$$

The strains can be defined as:

$$\left.\begin{aligned} e_x &= \frac{1}{2} w_{,x}^2 \end{aligned}\right\}$$

$$\varepsilon_y = \frac{1}{2} w_{,y}^2 \tag{7}$$

$$\varepsilon_{xy} = \frac{1}{2} w_{,x} w_{,y}$$

where $w(x, y)$ represents the displacement in z-direction. Now, the element with N nodes are accepted, the displacement for these elements can be expressed:

$$w = [N]_{1\times 3N}\{d\} \tag{8}$$

where [N] is the shape function of the element,

$\{d\} = \lfloor w_1\, w_{,x1}\, w_{y1} \cdots \quad w_N\, w_{,xN}\, w_{,yN} \rfloor$ is the matrix of the degree of freedom

From (8), the derivative formula will be:

$$\begin{Bmatrix} w_{,x} \\ w_{,y} \end{Bmatrix} = [G]_{2\times n}\{d\}_{n\times 1} \tag{9}$$

where n=3N is the number of degree of freedom for each element,

[G] is the derivative of the shape function. If N_X, N_Y, and N_{xy} are not related to the displacement, W, then the work done by these forces:

$$\pi_s = \int_A \left(\frac{1}{2} w_{,x}^2 N_X + \frac{1}{2} w_{,y}^2 N_Y + w_{,x} w_{,y} N_{XY} \right) dA \tag*{.(10)}$$

the matrix in Esq. (10) cab be expressed by the other form:

$$\pi_s = \frac{1}{2} \iint \begin{Bmatrix} w_{,x} \\ w_{,y} \end{Bmatrix}^T \begin{bmatrix} N_X & N_{XY} \\ N_{XY} & N_Y \end{bmatrix} [G] dxdy \tag{11}$$

Substituting Esq.(9) into Esq.(11) , the new equation can be obtained :

$$\pi_s = \frac{1}{2} \{d\}^T [K_a] \{d\} \tag{12}$$

where

$$[K_s] = \iint [G]^T \begin{bmatrix} N_X & N_{XY} \\ N_{XY} & N_Y \end{bmatrix} [G] dxdy \tag{13}$$

$[K_s]$ is call the negative stiffness matrix of the plate. In Equ.(13) , $[K_s]$ is observed through the contribution of the force N_x , N_y , and N_{xy}. If these forces are compressible, the $[K_s]$ will be negative, the stiffness of the plate will be going down. If the compressive force is continuingly increase to make the stiffness of plate zero, the buckling load of the plate will be observed.

2. Nonlinear Buckling Analysis

The buckling load calculated from the linear buckling analysis is an ideal buckling strength based on the linear elastic theory. Generally, it can only predict the upper bound of the buckling load of the structure, and generally the upper bound value is higher than that of the experimental results. Especially in the case of the laminate with the small de-lamination length, the buckling load calculated from the linear buckling theory is too higher. For getting more reasonable results about the engineering buckle problem, the lower bound of the buckling load of the structure must be calculated through the nonlinear buckling analysis. As though the linear buckling analysis can only get the upper bound of the buckling load, it is easily to reach the solution convergence and get the critical buckling load. It can save lots of time compared with the nonlinear buckling analysis. It also can apply the linear buckling analysis to investigate the buckling mode before the nonlinear buckling analysis is performed.

In general, there have two methods to do the nonlinear buckling analysis. In nonlinear buckling analysis, the large deflection is along with the buckling of the structure and the phenomena of nonlinear geometry will be observed. Therefore, the above theory included the large deflection effect is thought as a nonlinear buckling analysis. In the analytical proceeding, the external force must be applied step by step to make sure reach the convergence. When the external fore reached a critical value and can't get the convergent solution, the critical buckling load is found. An important idea is that the de-lamination of the composite laminate will be modified by the surface to surface contact element. The contact element will provide the nodes along the de-lamination cannot interfere each other and can get more perfect solution compared with the experimental observations. In this research, the buckling load will be calculated from the theoretical method, a linear finite element buckling analysis and nonlinear finite element buckling analysis and compared with each other.

3. The Buckling Analysis Of Column

In this section, a long steel column having the rectangular cross section will be analyzed. The column is fixed at the bottom and an unit compressive load is applied at the top, see Fig.6 In Fig.6 the length of the column is L, the width is b , and the height is h. All dimensional unit is cm, and the applied load is N. So the unit of the critical buckling load is still Newton. The geometric dimensions are listed in the table 1.

The Young's model of steel=30*10^6 psi, Poisson's ratio=0.3, and the moment of inertia :

$$I = \frac{bh^3}{12} = 5.208 \times 10^{-3} in^4 = 209.3 \times 10^{-3} cm^4 = 0.2093 \ cm^4$$

The critical buckling lo ad: $P_{cr} = \frac{p^2 EI}{4C^2} = 38.533(lb)$

The boundary conditions and applied load for three different models are the same, only 1-D model is shown in Figs. 6 and 7.

The mode shape for three different models is the same, therein, only the mode shapes of 1-D model are shown in Figs. 8-12. The buckling load for five different modes is listed in Table 2.

The Comparison between the results obtained from 1-D, 2-D, and 3-D finite element modes and that of the theoretical solutions are summarized in the Table 3.

From Table 2 and Table3, the results for the first critical bucking load obtained from the closed solutions are the same as that of the finite element analysis obtained from 1-D, 2-D or 3-D models. For the mode from 2 to 4, the critical buckling loads obtained from 2-D are very closed to that from 3-D. The results observed from 1-D model have big deviation from that calculated from 2-D ad 3-D models. Therefore, the 3-D finite element model is more suitable to do the buckling analysis.

4. The Buckling Analysis Of Delaminated Composite

From the above analysis, the 3-D finite element analyses are better to analyze the buckling analysis. In real case, the laminated composite with the pre-delamination can only be analyzed by using the 3-D finite element model because the crack between two sub-laminates are easily created. In this section, the experimental data would be referred to the reference 1. The geometric shape dimensions are plotted in Fig. 13.

Four half-circle de-laminations are created in the laminated composite beam. The material applied here is XAS/914 c and its ply orientations are $\{+45° / 0° / 0° / 90° / 0° - 45\%0\}_s$.

In reference 1, four different specimens are designed to perform the experiments. Four different specimens have assigned different numbers: SCB3-5, SCB 3-6, SCB3-7 and SCB3-8 which included the different de-lamination lengths and locations. In the tests, the bottom of the laminated beam is fixed and the unit load is to apply at the top of the pre-de-lamination beam. In Figure 12, the cones section of the de-lamination beam is the rectangular, b is the length of the beam, c is the width, t is the thickness, a is the radius of the half-circle de-lamination area, and d is the distance between the end edge of beam to the cent of the de-lamination area. All dimensional unit is mm, the force unit is N, the unit of the buckling load will be N/mm. The following table listed all geometric dimensions for four different specimens.

The material properties of composite material is show in the following

$E_X = 130Gpa$, $E_Y = 12Gpa$, $G_{XY} = 4.8Gpa$,*and* $U_{XY} = 0.28$

The critical load obtained from the experiment for the above specimens is listed in the following, The buckling load for the same specimen calculated from the closed form solution {see ref.1} is 132.9N/mm.

5. Finite Element Analysis For Delaminated Composite

The boundary conditions and applied load on these four specimens are the same, only the finite element model for the specimen of SCB3-5 is show in Fig. 14. The exaggeration of the applied load on the top of the specimen is plotted in Figure 15. The buckling analyses are performed for the laminate plate without de-lamination and with de-laminations. For comparison, all of the analysis will get 6 modes and buckling load. Table 6 would present the 6-buckling load for the composite laminate without the de-lamination. The results from the other two analyses are summarized in Tables 7 and 8.

The results from the linear buckling analysis for 4 different specimens are listed in Table 7. Table 8 would list the buckling load of those four specimens calculated from the non-linear buckling load.

The buckling load of specimen without de-lamination is generally higher 25% then that of the specimen with d lamination. Also the buckling load is increasing for higher buckling mode. The interesting results observed in Tables 7 and 8 are that the buckling load are almost the same and doesn't matter with the buckling analysis or nonlinear buckling analysis. The big difference between linear buckling analysis and nonlinear buckling analysis came from the deformation in the de-lamination area.

The load deformation of the linear buckling analysis is shown in Fig. 16. The deformation of the elements is along the de-lamination area that there has no any contact element between them.

The linear buckling analytical results showed that the element will interfere with each other and it is not existed in real case. Fig. 17 showed the local deformation obtained by using the nonlinear buckling analysis and it is obvious that the local buckling would appear but the element didn't cross with each other. More discussions about the results shown in Table 8 will be made in the following section.

The specimens of SCB3-8 have the same de-lamination locations, but the de-lamination area of SCB3-5 is bigger than that of SCB3-8 (see Table 4). The results showed that the small buckling load would be observed when the de-lamination area is bigger. The buckling load for the higher mode would get a larger and the loading deviation between two cases become larger as the buckling mode is becoming bigger. The specimen of SCB3-6 and SCB3-7 has the same de-lamination locations, but the de-lamination area of SCB3-6 is bigger than that of SCB3-7. The de-lamination area of specimen SCB3-6 is located at 5/6 plys and 9/10th plys, and that of specimen SCB3-5 is located at $6/7^{th}$ plys and $8/9^{th}$ plys. The distance in the thickness direction between the de-lamination of SCB3-6 is bigger than that the laminate of SCB3-5 had. The results showed that the de-lamination areas were too close in the multiple de-lamination laminate would reduce their buckling resistance capacity. The buckling modes of the multi-delamination laminate with the semi-circle de-lamination shape are shown in Figs.18 to 23 that the first 6 mode shapes are plotted.

Summarizations of the above analytical results with the theoretical and experimental data are shown in the following.

From the above calculations, the results obtained from the finite element analysis agree very well with that of the theoretical solutions. But big deviations are also observed among the experimental data, theoretical solution and results obtained from finite element analysis. The results obtained from finite element analysis are more closed to the experimental data than that of the theoretical analysis. The theoretical analysis cannot match with the experimental data because more simplification assumptions are held in the theoretical analysis. Therefore, the next sections will only apply the finite element analyses to do the buckling analyses and compare with the experimental data.

III. Mesh Density Neighboring The De-lamination Area Effect On The Buckling Load

Based on the above discussions, the results obtained from the linear and nonlinear element analysis have much deviation from the experimental data. Based on the previous analytical results, the linear buckling analysis and nonlinear buckling analysis will get the same buckling load and global buckling mode shape except the local buckling deformation and computer running time. The computer running time for the nonlinear buckling analysis may spend 20 times of the linear buckling analysis. For reducing the running time to evaluate more reasonable critical buckling load, the linear buckling analysis will be executed in this section. The Fig. 24 is the local mesh included the de-lamination area and the neighboring area. In the previous section, 10 elements in 33 cm length were created in the de-lamination neighboring area. To get more reliable solution, the length of the de-lamination neighboring area included 10 elements will be shrunken to be 20mm and 5mm. After the length of the de-lamination neighboring area become s maller, it meant that the mesh density becomes higher and didn't affect the other. The results are shown in Fig. 28 that the higher mesh density neighboring the de-lamination area can get better results compared with the experimental data. And it is normal that the finite element solutions from higher mesh density are far from the theoretical results. From these results, the mesh density neighboring the de-lamination area must be dense and the mesh density effect must beconsidered.

IV. De-lamination Area Considerations

The structure subjected to the foreign force may cause the damage area and de-lamination area. Generally the de-lamination area is irregular in the laminate and it is hard to do the analysis or modeled. For simplifying the analysis, the regular shape of the de-lamination area is assumed. In the section, different de-lamination area shape is considered here to investigate its effect on the buckling load. Three different de-lamination shapes such assemicircle, triangle, and rectangle are assumed. The semicircular de-lamination shape is already studied in the previous section and become the basic data. For triangular and rectangular de-lamination areas are also assumedexisted at the different plysas the same as the description in Table 4. These three different de-lamination shapes in the finite element model are shown in Figs. 26, 27, and 28.

The six buckling load were summarized in Tables 13 to 16. The results showed that the rectangularde-lamination area would get the lower buckling load. The buckling load of each mode is very closed for the semicircular and triangular de-lamination area. Comparisons for the different shapede-lamination area are basically that the rectangular de-lamination area are bigger than that of semicircular ad triangular shape would result in the lower buckling load due to a little bigger de-lamination area and not affected by the de-lamination location and shape.

V. Conclusions

1. In the buckling analysis, the results obtained from the finite element analysis are agree very well with that of experimental data
2. In theoretical analysis, the 1-D geometric dimension one areassumed, and in real care 3-D geometric is general, there fore theoreticalsalvation didn't consider real geometric effect and why. The result calculated from thecortical method can't match with the results obtained from theexperimental test and 3-D finite element analysis. But the results obtained from 1-D finite element analysis can completely with that of theoretical analysis.
3. The buckling strength of the laminate without the de lamination is higher than that of the laminate with the de lamination.
4. The buckling strength of the laminate will dependan the de lamination area and not strength related with the de lamination location and shape.
5. For getting the best results from the finite element analysis, the mesh density of the area near or neigh boring the de lamination must be dense. The mesh density can be determined from the finite element analysis.
6. The finite element analysis can get very good results compared with the experimental data
7. The buckling load wouldbecome smaller when de laminations are closed to the surface of the laminate.

VI. References

(1) Mustafa Aslan, and William M. Banks (1998), "The effect of multiple de-lamination on post-buckling behavior of laminated composite plates," Composite Structures;42:pp. 1-12.

(2) Kachanov, L. M. (1976), "Separation of Composite Materials", Mekh. Polim. No.5, pp. 918-922.

(3) Chai, H., Babcock, C. D., and Knauss, W. G., (1981), "One Dimensional Modeling of Failure in Laminate Plates by Delamination Buckling", International Journal of Solids and Structures", Vol.17, No.11, pp. 1069-1083.

(4) Bottega, W. J. and Maewal, A., (1983), "Delamination Buckling And Growth in Laminates", Journal of Applied Mechanics, Vol.50, pp.184-189.

(5) Vizzini, A. J. and Lagace, P. A., (1987), "The Buckling of a Delaminated Sublaminate on an Elastic Foundation", Journal of Composite Materials, Vol.21, pp.1106-1117.

(6) Wang, J. T., Cheng, S. H., and Lin, C. C., (1995), "Local Buckling of Delaminated Beams and Plates Using Continuous Analysis", Journal of Composite Materials, Vol.29, No.10, pp.1374-1402.

(7) Chen, H. P., (1993), "Transverse Shear Effects on Buckling and Postbuckling of Laminated and Delaminated Plates", AIAA Journal, Vol.30, No.1, pp.163-169.

(8) Lee, J., Gurdal, Z., and Griffin, O. H., Jr., (1995), "Postbuckling of Laminated Composite with Delaminations", AIAA Journal, Vol.33, No.10, pp.1963-1970.

(9) Kyoung, W. M. and Kin, C. G., (1995), "Delamination Buckling And Growth of Composite Laminate Plates with Transverse Shear Deformation", Journal of Composite Materials, Vol.29, No.15, pp.2047-2068.

(10) Kardomateas, G. A., (1993), "The Initial Post-buckling and Growth Behavior of Internal Delaminations in Composite Plates", Journal of Applied Mechanics, Vol.60, pp.903-910.

(11) Chattopadhyay, A. and Gu, H., (1994), "New Higher Order Plate Theory in Modeling Delamination Buckling of Composite Laminates", AIAA Journal, Vol.32, No.8, pp.1709-1716.

(12) Davidson, B. D. and Krafchak, T. M., (1995), "A Comparison of Energy Release Rates for Locally Buckled Laminates Containing Symmetrically and Asymmetrically Located Delaminations", Journal of Composite Materials, Vol.29, No.6, pp.700-713.

(13) Kutlu, Z. and Chang, F. K., (1992), "Modeling Compression Failure of Laminatred Composites Containing Multiple Through-The-Width Delaminations", Journal of Composite Materials, Vol.26, No.3, pp.350-387.

(14) Adan, M., Sheinman, I., and Altus, E., (1994), "Buckling of Multiply Delaminated Beams", Journal of Composite Materials, Vol.28, No.1, pp.77-90.

(15) Wang, J. T., Pu, H. N., and Lin, C. C., (1997), "Buckling of Beam-Plates Having Multiple Delaminations", Journal of Composite Materials, Vol.31, No.10, pp.1002-1025.

(16) Shivakumar, K. N. and Whitcomb, J. D., (1985), "Buckling of a Sublaminate in a Quasi-Isotropic Composite Laminate", Journal of Composite Materials, Vol.19, pp.2-18.

(17) Chai, H. and Babcock, C. D., (1985), "Two-Dimensional Modeling of Compressive Failure in Delaminated Laminates", Journal of Composite Materials, Vol.19, pp.67-98.

(18) Yeh, M. K. and Tan, C. M., (1994), "Buckling of Elliptically Delaminated Composite Plates", Journal of Composite Materials, Vol.28, No.1, pp.36-52.

(19) Kassapoglou, C., (1998), "Buckling, Post-buckling and Failure of Elliptical Delaminations in Laminates under Compression", Composite Structures, Vol.9, pp.139-159.

(20) Whitcomb, J. D. and Shiva Kumar, K. N., (1998), "Strain-Energy Release Rate Analysis of Plates with Postbuckled Delamination", Journal of Composite Materials, Vol.23, pp.714-734.

(21) Woo-Min Kyoung, Chun-Gon Kim, Chang-Sun Hong, (1999), "Buckling and postbuckling behavior of composite cross-ply laminates with multiple delaminations," Composite Structures, 43:pp. 257-274.

(22) Timoshenko, S., and Gere, J. M., (1961), "Theory of Elastic Stability," 2nd Edition, McGraw-Hill Book Co., Inc., New York,

91 年 9 月 4 日投稿
91 年 9 月 30 日接受

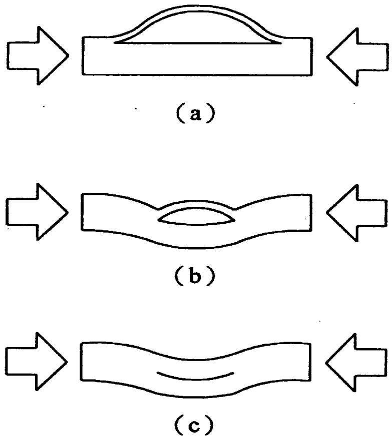

Figure 1 the buckling mode (a)local mode(b)mixed mode(c)global mode [3]

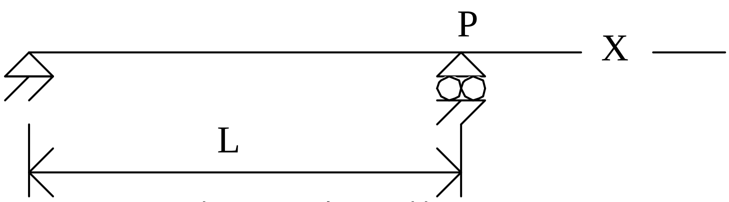

Figure 2 column with supports

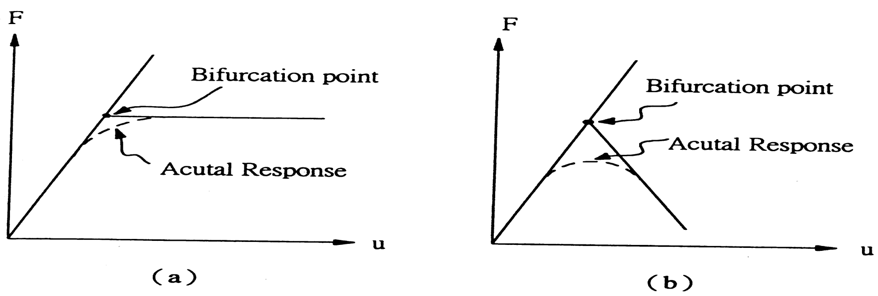

Figure 3 the solving procedures for the buckling analysis

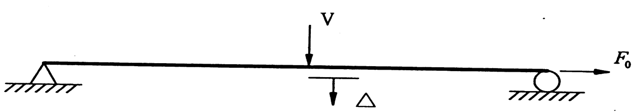

Figure 4 the applied forces in the simple support beam

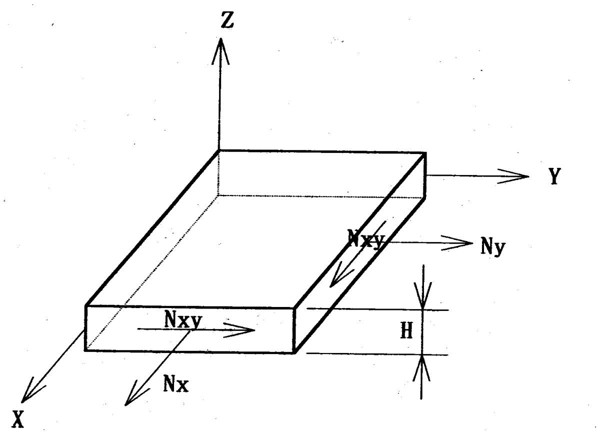

Figure 5 the applied forces in XY plane for the plate

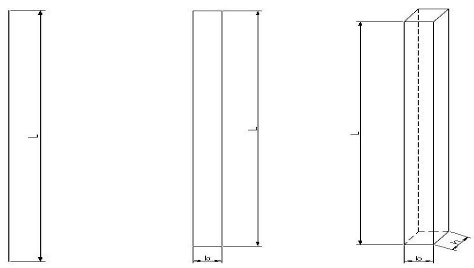

(a) (b) (c)

Figure 6 the model of the column (a) 1-D model (b) 2-D model (c) 3-D model

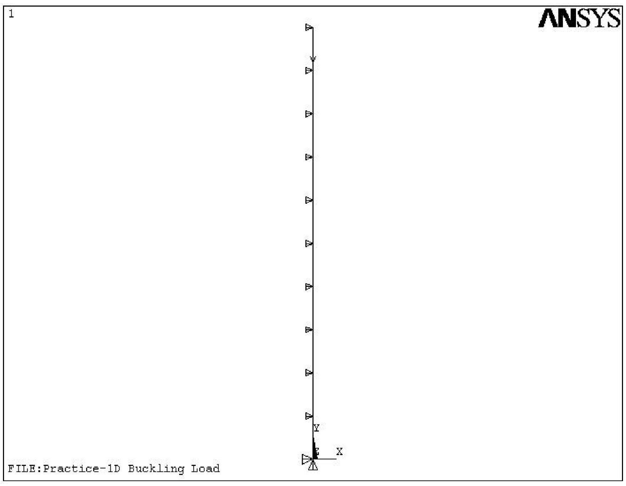

Figure 7 the boundary conditions and applied load of 1-D model

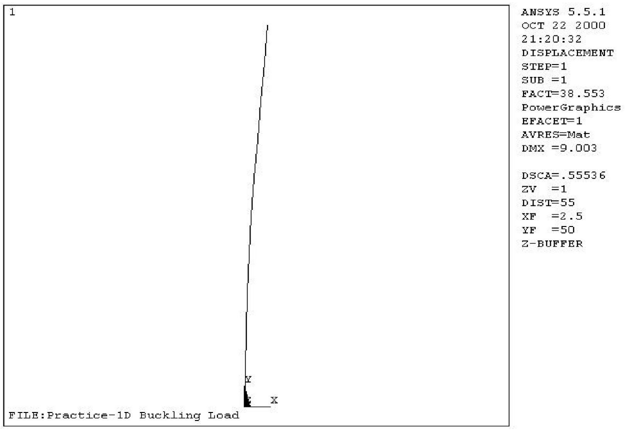

Figure 8 the first buckling mode with the buckling load of 175.4 N

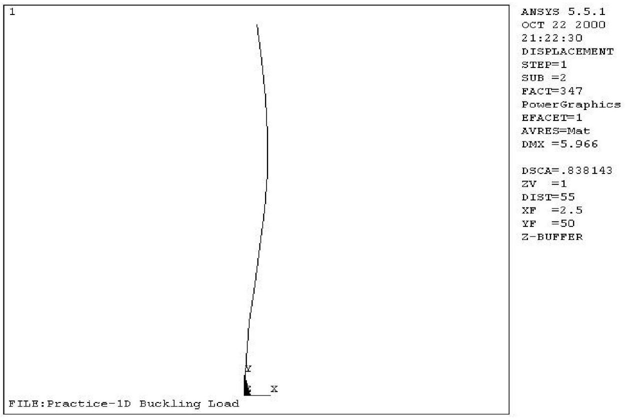

Figure 9 the 2nd buckling mode with the buckling load of 1578.9 N

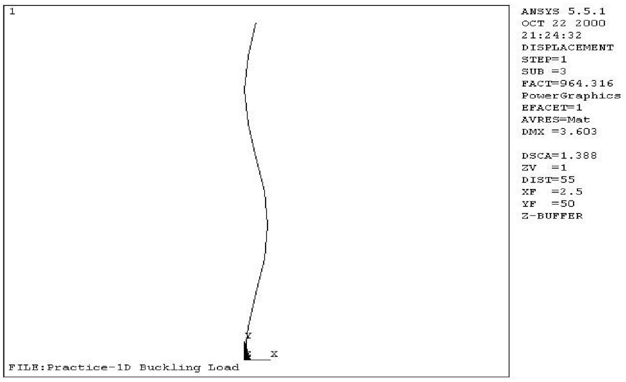

Figure 10 the 3rd buckling mode with the buckling load of 4387.7 N

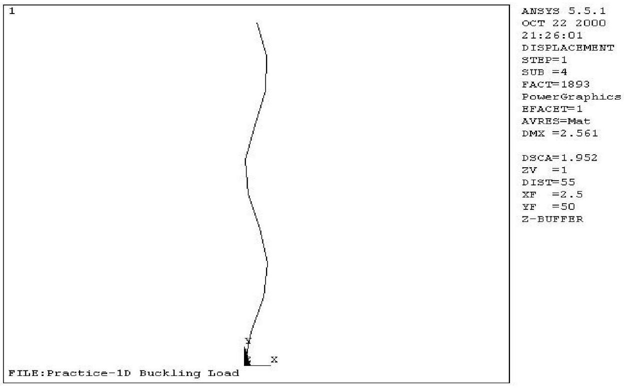

Figure 11 the 4th buckling mode with the buckling load of 8611.8 N

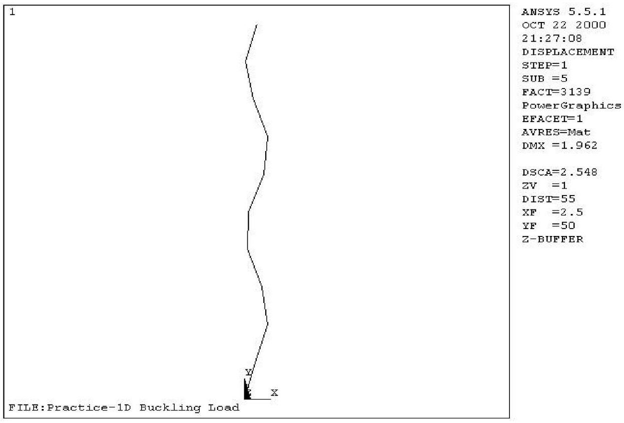

Figure 12 the 5th buckling mode with the buckling load of 21453.7 N

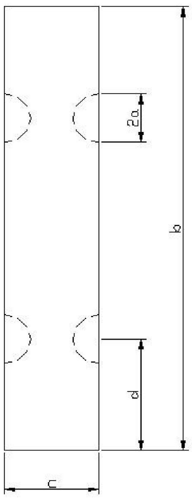

Figure 13 the composite specimen with four half-circle de-lamination areas

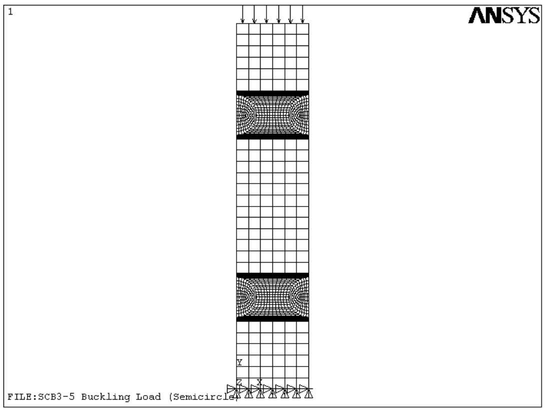

Figure 14 the finite element model for specimen of SCB3-5

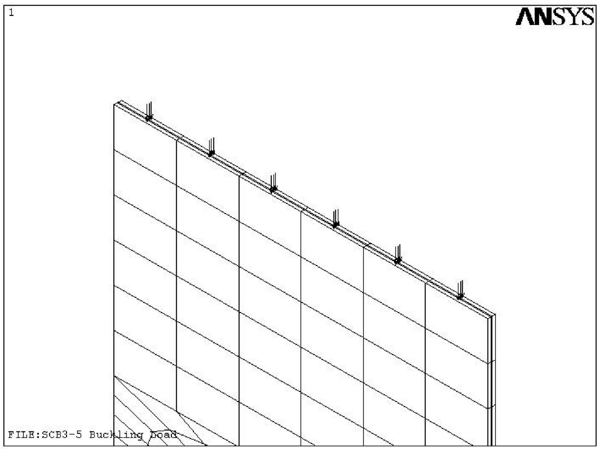

Figure 15 the applied forces in the model for specimen of SCB3-5

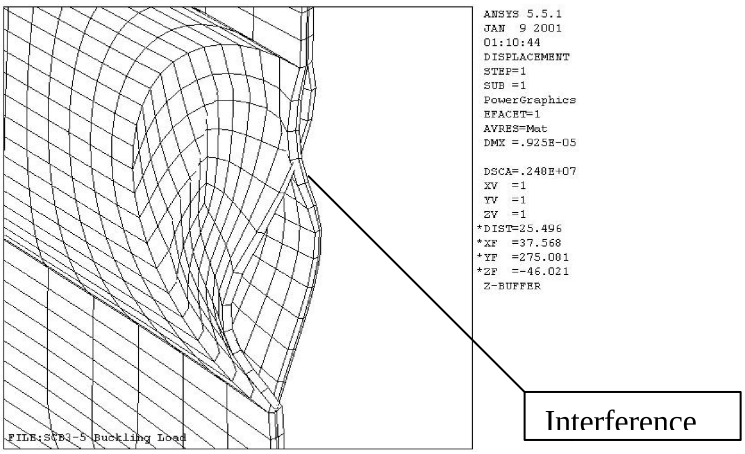

Figure 16 the interference between elements in linear buckling analysis

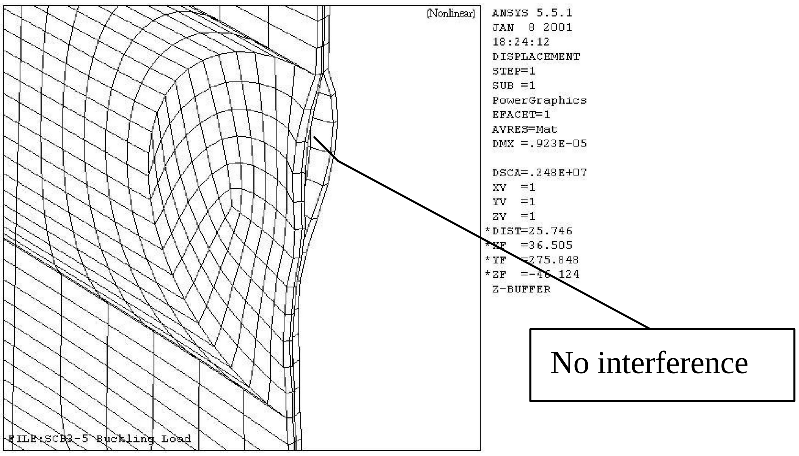

Figure 17 no interference between elements in nonlinear buckling analysis

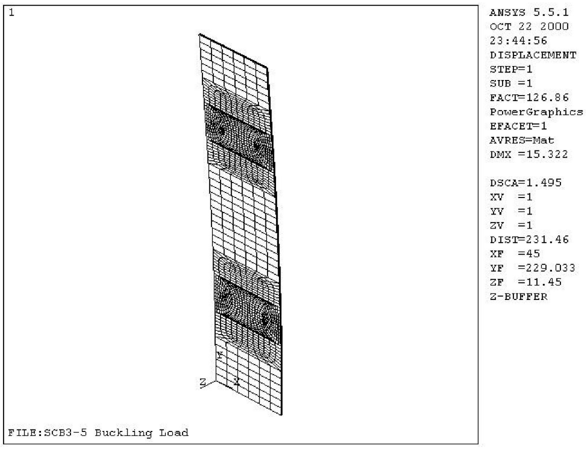

Figure 18 the first mode of the specimen of SCB3-5

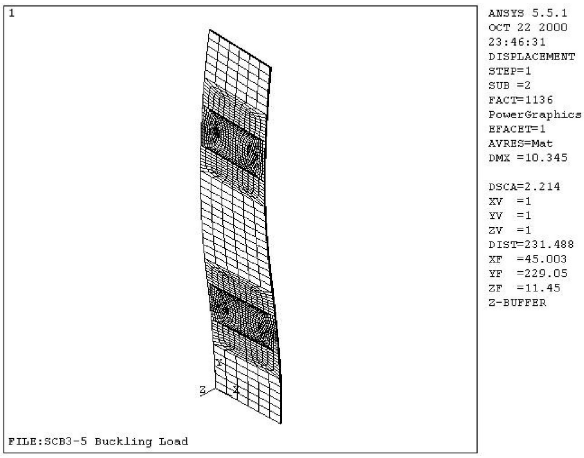

Figure 19 the second mode of the specimen of SCB3-5

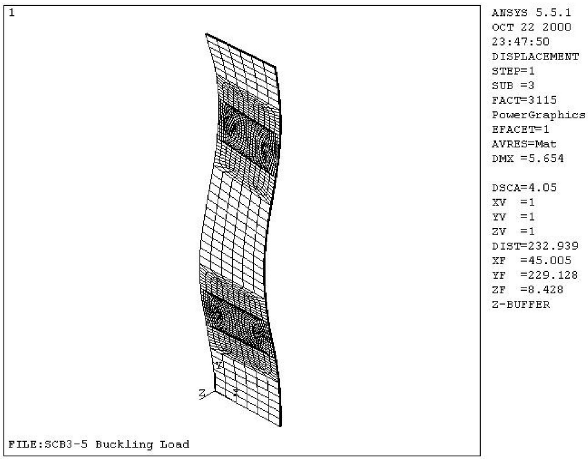

Figure 20 the third mode of the specimen of SCB3-5

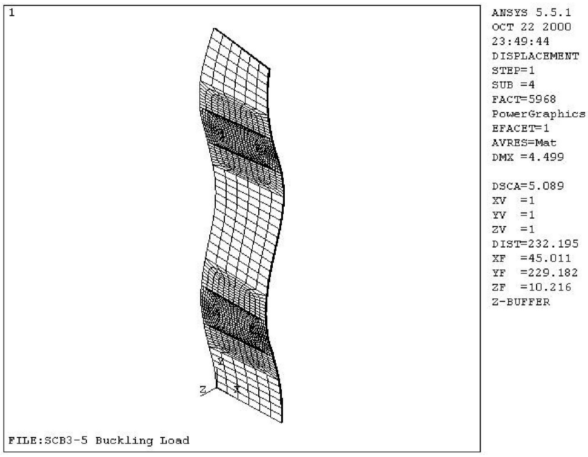

Figure 21 the fourth mode of the specimen of SCB3-5

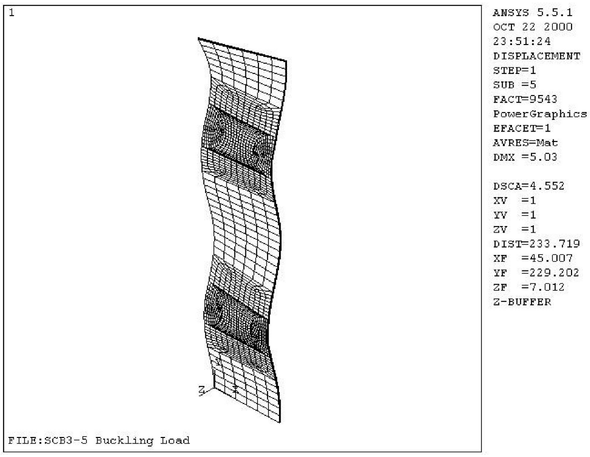

Figure 22 the fifth mode of the specimen of SCB3-5

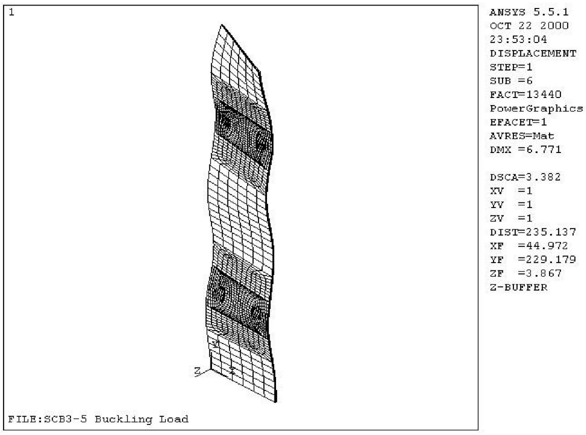

Figure 23 the sixth mode of the specimen of SCB3-5

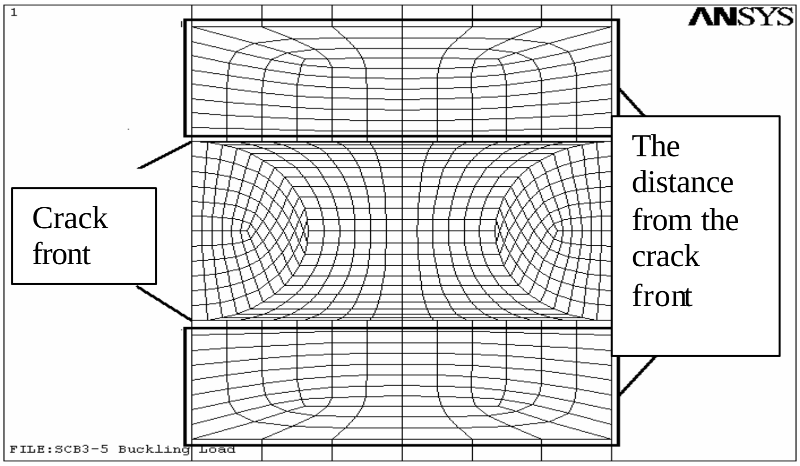

Figure 24 the distance of the de-lamination neighboring area from the crack front

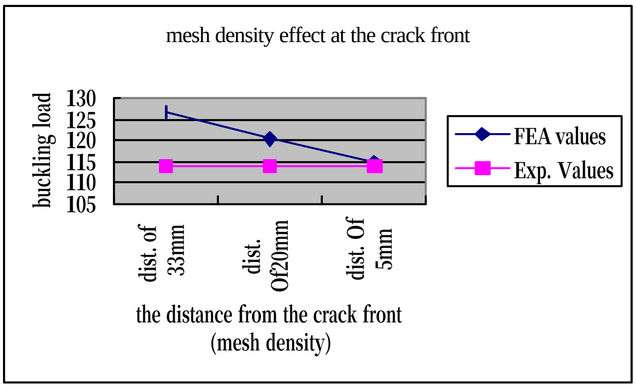

Figure 25 the comparison of the buckling load of specimen of SCB3-5 with different mesh density

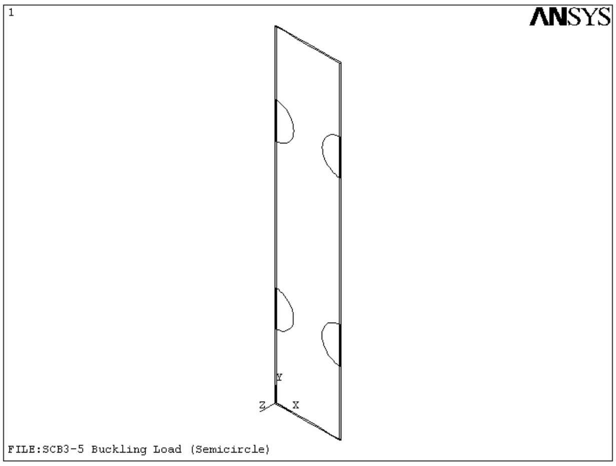

Figure 26 the specimen with the half-circle de-lamination area

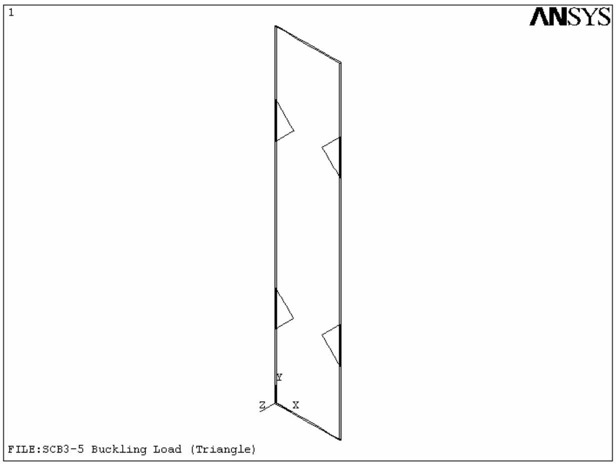

Figure 27 the specimen with the triangular de-lamination area

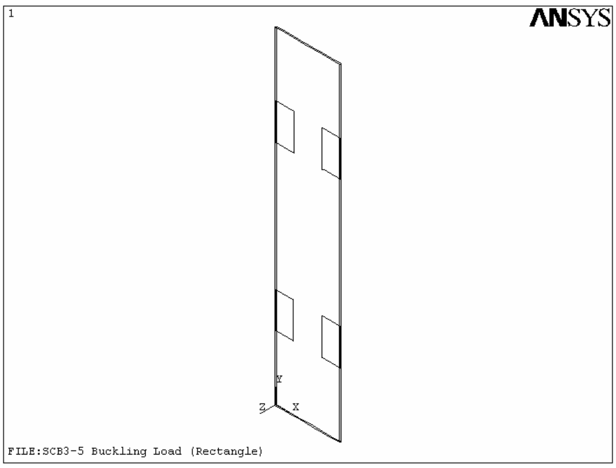

Figure 28 the specimen with the rectangular de-lamination area

Table 1 Geometric Dimensions of Column with the square cress-section

column (L)	width (b)	height (h)	cross-section area
2540cm	1.27cm	1.27cm	1.613cm^2

Table 2 The buckling load of five modes (N)

	1-D	2-D	3-D
Mode 1	175.4	176.1	177.4
Mode 2	1578.9	1639.9	1655.9
Mode 3	4387.7	4886.3	4959.9
Mode 4	8611.8	10712.1	10960.5
Mode 5	21453.7	20825.4	21530.1

Table 3 The Comparisons between different models (unit=N)

	Theoretical solution	FEM	Err (%)
1-D	175.4	175.4	0
2-D	175.4	176.1	0.481
3-D	175.4	177.4	1.141

Table 4 Geometric Dimensions of Four Specimens

	SCB3-5	SCB3-6	SCB3-7	SCB3-8
Specimen length (mm)	458	458	458	458
Specimen width (mm)	90	90	90	90
Specimen thickness (mm)	1.75	1.75	1.75	1.75
De lamination length (mm)	25	25	18.75	18.75
The location of De lamination	6/7th plys and 8/9th plys	5/6th plys and 9/10th plys	5/6th plys and 9/10th plys	6/7th plys and 8/9th plys

Table 5 Experiment critical load

	SCB3-5	SCB3-6	SCB3-7	SCB3-8
Buckling load (N/mm)	113.9	116.6	110.7	114.9

Table 6 The buckling load for the specimen without the de-lamination

load / Mode	Critical load (N/mm)
Mode1	166.22
Mode2	1494.1
Mode3	4139.6
Mode4	8081.4
Mode5	13286
Mode6	19694

Table 7 The buckling load (linear buckling analysis)

	SCB3-5 (N/mm)	SCB3-6 (N/mm)	SCB3-7 (N/mm)	SCB3-8 (N/mm)
Mode1	126.86	138.7	141.14	129.39
Mode2	1136.4	1240.6	1264.5	1160.4
Mode3	3114.5	3391.1	3477.1	3198.7
Mode4	5967.8	6478.2	6683.6	6159.5
Mode5	9542.7	10262	10639	9841.6
Mode6	13440	14173	14733	13853

Table 8 the buckling load (nonlinear buckling analysis)

	SCB3-5 (N/mm)	SCB3-6 (N/mm)	SCB3-7 (N/mm)	SCB3-8 (N/mm)
Mode1	126.87	138.74	141.16	129.39
Mode2	1136.5	1241	1264.7	1160.5
Mode3	3115	3393	3477.8	3198.9
Mode4	5968.9	6484.4	6685.6	6159.8
Mode5	9545.1	10281	10643	9842.2
Mode6	13444	14223	14743	13853

Table 9 the results comparison between different methods (unit=N/mm)

	Theory	Experimental data	Linear analysis	Nonlinear Analysis
SCB3-5	132.9	113.9	126.86	126.87
SCB3-6	132.9	116.6	138.7	138.74
SCB3-7	132.9	110.7	141.14	141.16
SCB3-8	132.9	114.9	129.39	129.39

Table 10 the error percentage of different methods (unit=%)

	Linear analysis and theory	Linear analysis and experimental data	Nonlinear Analysis and theory	Nonlinear Analysis and experimental data
SCB3-5	4.545	10.216	4.537	10.223
SCB3-6	4.364	15.934	4.394	15.958
SCB3-7	6.2	21.567	6.215	21.578
SCB3-8	2.641	11.199	2.641	11.199

Table 11 the buckling load comparison from three methods (unit=N/mm)

	Close form solution	Experimental values	Re-analysis of FEA
SCB3-5	132.9	113.9	114.73
SCB3-6	132.9	116.6	128.59
SCB3-7	132.9	110.7	127.94
SCB3-8	132.9	114.9	113.66

Table 12 the error percentage from three methods (unit：%)

	Re-analysis of FEA/closed form solution	Re-analysis of FEA/experimental values
SCB3-5	13.672	0.723
SCB3-6	3.243	9.324
SCB3-7	3.732	13.475
SCB3-8	14.477	1.091

Table 13 the buckling load of specimen SCB3-5 with different de-lamination shapes (unit=N/mm)

	Semicircle	Triangle	Rectangle
Mode 1	114.73	113.78	111.43
Mode 2	1030.9	1024.9	997.25
Mode 3	2818	2822.6	2718.7
Mode 4	5387.3	5471.4	5172.4
Mode 5	9098.4	9141.4	8349.5
Mode 6	13049	13307	11686

Table 14 the buckling load of specimen SCB3-6 with different de-lamination shapes (unit=N/mm)

	Semicircle	Triangle	Rectangle
Mode 1	128.59	127.51	126.17
Mode 2	1152.4	1145.6	1124.6
Mode 3	3148.2	3153.4	3044.1
Mode 4	6006.1	6094.8	5714.9
Mode 5	9873.9	10001	8940.1
Mode 6	13827	14227	11781

Table 15 the buckling load of specimen SCB3-7 with different de-lamination shapes (unit=N/mm)

	Semicircle	Triangle	Rectangle
Mode 1	127.94	127.3	126.49
Mode 2	1150.3	1145.6	1132.5
Mode 3	3168.7	3166.6	3096.2
Mode 4	6129.4	6157.2	5903.3
Mode 5	10105	10124	9452.7
Mode 6	14381	14476	12950

Table 16 the buckling load of specimen SCB3-8 with different de-lamination shapes (unit=N/mm)

	Semicircle	Triangle	Rectangle
Mode 1	113.66	113.08	111.69
Mode 2	1024.7	1020.3	1003.7
Mode 3	2826.4	2825.2	2761.1
Mode 4	5486.3	5516.3	5323.3
Mode 5	9209.7	9205.2	8710.5
Mode 6	13436	13497	12454